

Design and Analysis of Exponential Taper Directional Coupler

Adnan Affandi and Yasser Gharbi

Elect. & Comp. Eng., Faculty of Eng. King Abdul Aziz University Jeddah, KSA
ygharbi999@yahoo.com

Abstract: Coupled exponential transmission lines in inhomogeneous media are analyzed. The solution is used to design microwave directional couplers. The designed couplers have much improved coupling characteristics compared with couplers using uniform lines.

[Adnan Affandi, Yasser Gharbi. **Design and Analysis of Exponential Taper Directional Coupler.** *Life Sci J* 2015;12(4):153-163]. (ISSN:1097-8135). <http://www.lifesciencesite.com>. 19

Keywords: Exponential Taper ; Directional Coupler

1. Introduction

Non-uniform transmission lines have considerable applications in microwave circuits such as resonators, transformers, matching sections and filters [1]. Normally the TEM mode of propagation in the non-uniform transmission line is described by its non-constant characteristic impedance which varies along the direction of propagation of electromagnetic waves. This property made the non-uniform transmission lines responses more superior than those of uniform ones.

Usually the exact network functions of general non-uniform transmissions except for view cases such as binomial transmission lines (including linear and parabolic tapers) exponential, Triangular and radial transmission lines [2].

Uniform & Non-uniform transmission lines could be isolated or coupled. Coupled uniform transmission lines are used in the realization of various types of microwave circuits i.e. filters, frequency discriminator, directional couplers, phase shifters and impedance transformers. Coupled non-uniform transmission line, by its nature of non-uniformity, offers additional design parameters to achieve the desired device performance, inherent impedance transformation capabilities and the possibility of the realization of a wide band components.

Therefore non-uniform transmission line directional couplers can provide both broad band capability and superior transmission responses than the uniform ones. These coupler may be served as a building blocks for phase shifters, mixers, multiplexers, balance and duplexers which are essential and required in multi-octave bandwidth antenna and broadband microwave systems.

2. Analysis of Lossy Exponential Transmission Line (CETL)

The relevant parameters of the exponential lossy coupled line which is shown in Fig. 1(a) can be easily

analyzed in terms of the even and odd modes concepts. When two signals of amplitude 1/2 and both are in phase, applied to ports (1) and (2), the even mode propagation is resulted. Similarly, if two signals of amplitude 1/2 and are output of phase, and are applied, the odd mode propagation is produced. Superposition of these two fundamental modes describes the behavior of the line. The even and odd mode inductances, resistances, conductances and capacitances are expressed as:

$$L_{e,o}(x) = L_{11}(x) + L_{12}(x) \quad (1)$$

$$R_{e,o}(x) = R_{11}(x) + R_{12}(x) \quad (2)$$

$$C_{e,o}(x) = C_{11}(x) \pm C_{12}(x) \quad (3)$$

$$G_{e,o}(x) = G_{11}(x) \pm G_{12}(x) \quad (4)$$

Where subscripts e and o defined before; and plus and minus signs refer to the even and odd modes respectively.

The parameters of the Lossy (CETL) are:

$$L_{e,o}(x) = L_{e,o} e^{\alpha_{e,o}x} \quad ; \quad R_{e,o}(x) = R_{e,o} e^{\alpha_{e,o}x}$$

$$C_{e,o}(x) = C_{e,o} e^{-\alpha_{e,o}x} \quad ; \quad G_{e,o}(x) = G_{e,o} e^{-\alpha_{e,o}x}$$

Where $\alpha_{e,o}$ is the even-odd exponential taper? The voltage $v(x,t)$ and the current $i(x,t)$ along the line are:

$$\frac{\partial v_{e,o}(x,t)}{\partial x} = - \frac{L_{e,o}(x) \partial i_{e,o}(x,t)}{\partial t} - R_{e,o}(x) i_{e,o}(x,t) \quad (5)$$

$$\frac{\partial i_{e,o}(x,t)}{\partial x} = - \frac{C_{e,o}(x) \partial v_{e,o}(x,t)}{\partial t} - G_{e,o}(x) v_{e,o}(x,t) \quad (6)$$

Where $L_{e,o}(x)$, $R_{e,o}(x)$, $C_{e,o}(x)$ and $G_{e,o}(x)$ are defined previously. Equation (5) and (6) can be written in phasor form as:

$$\frac{dV_{e,o}}{dx} = -(j\omega L_{0e,o} + R_{0e,o})e^{\alpha_{e,o}x} * I_{e,o} \quad (7)$$

$$\frac{dI_{e,o}}{dx} = -(j\omega C_{0e,o} + G_{0e,o})e^{\alpha_{e,o}x} * V_{e,o} \quad (8)$$

Further differentiation of equations (7) and (8) w.r.t x yield the linear second order differential equations for the even and odd mode lines voltages and currents as:

$$\frac{d^2V_{e,o}}{dx^2} = -(j\omega L_{0e,o} + R_{0e,o})[\alpha_{e,o}e^{\alpha_{e,o}x} * I_{e,o} + e^{\alpha_{e,o}x} \frac{dI_{e,o}}{dx}] \quad (9)$$

$$\frac{d^2I_{e,o}}{dx^2} = (j\omega C_{0e,o} + G_{0e,o})[\alpha_{e,o}e^{-\alpha_{e,o}x} * V_{e,o} - e^{-\alpha_{e,o}x} \frac{dV_{e,o}}{dx}] \quad (10)$$

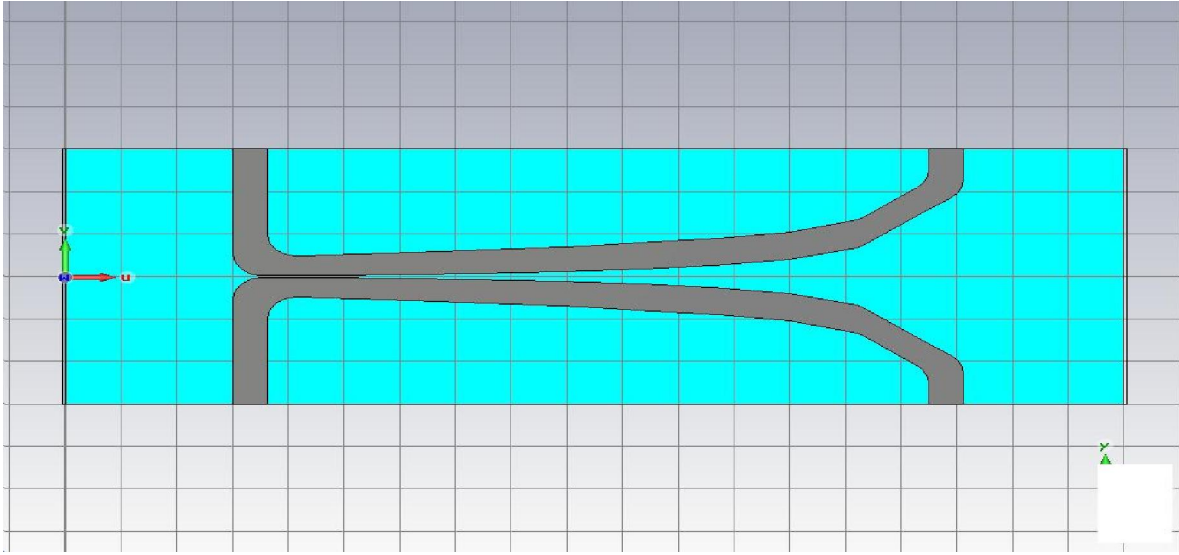


Fig.1 Exponential directional coupler layout

The solution of equations (9) and (10) can be written in the following form:

$$V_{e,o}(x) = V_{1e,o}^+ e^{\frac{\alpha_{e,o}x}{2}} e^{-j\beta_{e,o}x} + V_{1e,o}^- e^{\frac{\alpha_{e,o}x}{2}} e^{j\beta_{e,o}x} \quad (11)$$

$$I_{e,o}(x) = \frac{V_{1e,o}^+}{Z_{e,o}(x)} e^{\frac{-\alpha_{e,o}x}{2}} e^{-j\beta_{e,o}x} - \frac{V_{1e,o}^-}{Z_{e,o}^*(x)} e^{\frac{-\alpha_{e,o}x}{2}} e^{j\beta_{e,o}x} \quad (12)$$

$\beta_{e,o}$ is the even and odd phase constant. Where

$$\beta_{e,o} = \sqrt{\beta_{e,o,0}^2 + \left(\frac{\alpha_{e,o}}{2}\right)^2}$$

$$\beta_{e,o,0} = \sqrt{(j\omega L_{0e,o} + R_{0e,o})(j\omega C_{0e,o} + G_{0e,o})}$$

$$Z_{e,o} = Z_{e,o,0} e^{\alpha_{e,o}x}$$

Where

$$Z_{e,o,0} = \sqrt{\frac{j\omega L_{0e,o} + R_{0e,o}}{(j\omega C_{0e,o} + G_{0e,o})}}$$

$$Z_{e,o}^* = \sqrt{\frac{j\omega L_{0e,o} + R_{0e,o}}{(j\omega C_{0e,o} + G_{0e,o})}} e^{j\theta_{e,o}}$$

where

$$\theta_{e,o} = \tan^{-1}\left(\frac{\alpha_{e,o}}{2\beta_{e,o}}\right)$$

By superposition of these two modes, the steady state solutions for the voltage and current waves on lines I and II in Fig. 1(b) are obtained as:

$$VI, II(x) = V_e(x) \pm V_o(x) \quad (13)$$

$$II, II(x) = I_e(x) \pm I_o(x) \quad (14)$$

The above equations shows that the total voltages and currents on the coupled line network are linear combination of the even and odd modes waves, of each line.

3. Determination of the ABCD Matrix

Expression for the ABCD matrix from the steady-state solution can be found as follows:

$$V_{1e,o}^+ = Z_{oe,oo} I_{1e,o}^+ \quad (15)$$

$$V_{1e,o}^- = -Z_{oe,oo}^* I_{1e,o}^- \quad (16)$$

atx = l

$$V_{2e,o} = V_{1e,o}^+ e^{\frac{\alpha_{e,o}l}{2}} e^{-j\beta_{e,o}l} + V_{1e,o}^- e^{\frac{\alpha_{e,o}l}{2}} e^{j\beta_{e,o}l} \quad (17)$$

⇒

$$V_{2e,o} = V_{1e,o}^+ e^{\frac{\alpha_{e,o}l}{2}} e^{-j\beta_{e,o}l} - I_{1e,o}^- Z_{oe,oo}^* e^{\frac{\alpha_{e,o}l}{2}} e^{j\beta_{e,o}l} \quad (18)$$

$$I_{2e,o} = \frac{V_{1e,o}^+}{Z_{oe,oo}} e^{\frac{-\alpha_{e,o}l}{2}} e^{-j\beta_{e,o}l} - I_{1e,o}^- e^{\frac{-\alpha_{e,o}l}{2}} e^{j\beta_{e,o}l} \quad (19)$$

equations (18) and (19) can be arranged in matrix form as:

$$\begin{bmatrix} V_{2e,o} \\ I_{2e,o} \end{bmatrix} = \begin{bmatrix} e^{\frac{\alpha_{e,o}l}{2}} e^{-j\beta_{e,o}l} & -Z_{oe,oo}^* e^{\frac{\alpha_{e,o}l}{2}} e^{j\beta_{e,o}l} \\ \frac{1}{Z_{oe,oo}} e^{-\frac{\alpha_{e,o}l}{2}} e^{-j\beta_{e,o}l} & e^{-\frac{\alpha_{e,o}l}{2}} e^{j\beta_{e,o}l} \end{bmatrix} \begin{bmatrix} V_{1e,o}^+ \\ I_{1e,o}^+ \end{bmatrix} \quad (20)$$

from the matrix properties $X = AY$ where A is a square matrix and AY is defined and

$$A_1^{-1}X \text{ is defined: } Y = A_1^{-1}X.$$

where

$$A_1 = \begin{bmatrix} e^{\frac{\alpha_{e,o}l}{2}} e^{-j\beta_{e,o}l} & -Z_{oe,oo}^* e^{\frac{\alpha_{e,o}l}{2}} e^{j\beta_{e,o}l} \\ \frac{1}{Z_{oe,oo}} e^{-\frac{\alpha_{e,o}l}{2}} e^{-j\beta_{e,o}l} & e^{-\frac{\alpha_{e,o}l}{2}} e^{j\beta_{e,o}l} \end{bmatrix}$$

$$A_1^{-1} = \frac{1}{Z_{oe,oo} + Z_{oe,oo}^*} \begin{bmatrix} Z_{oe,oo} e^{-\frac{\alpha_{e,o}l}{2}} e^{j\beta_{e,o}l} & Z_{oe,oo} Z_{oe,oo}^* e^{\frac{\alpha_{e,o}l}{2}} e^{j\beta_{e,o}l} \\ -e^{-\frac{\alpha_{e,o}l}{2}} e^{-j\beta_{e,o}l} & Z_{oe,oo} e^{\frac{\alpha_{e,o}l}{2}} e^{-j\beta_{e,o}l} \end{bmatrix}$$

$$\begin{bmatrix} V_{1e,o}^+ \\ I_{1e,o}^+ \end{bmatrix} = A_1^{-1} \begin{bmatrix} V_{2e,o} \\ I_{2e,o} \end{bmatrix} \quad (21)$$

The second part of this solution is to calculate $\begin{bmatrix} V_{1e,o}^- \\ I_{1e,o}^- \end{bmatrix}$ and then add to equation (21). from equations (15), (16), (17) and (18)

$$V_{2e,o} = Z_{oe,oo} I_{1e,o}^+ e^{\frac{\alpha_{e,o}l}{2}} e^{-j\beta_{e,o}l} + V_{1e,o}^- e^{-\frac{\alpha_{e,o}l}{2}} e^{j\beta_{e,o}l} \quad (22)$$

$$I_{2e,o} = I_{1e,o}^+ e^{-\frac{\alpha_{e,o}l}{2}} e^{-j\beta_{e,o}l} - \frac{V_{1e,o}^-}{Z_{oe,oo}^*} e^{-\frac{\alpha_{e,o}l}{2}} e^{j\beta_{e,o}l} \quad (23)$$

equations (22) and (23) can be arranged in matrix form as:

$$\begin{bmatrix} V_{2e,o} \\ I_{2e,o} \end{bmatrix} = \begin{bmatrix} Z_{oe,oo} e^{\frac{\alpha_{e,o}l}{2}} e^{-j\beta_{e,o}l} & e^{\frac{\alpha_{e,o}l}{2}} e^{j\beta_{e,o}l} \\ e^{-\frac{\alpha_{e,o}l}{2}} e^{-j\beta_{e,o}l} & -\frac{1}{Z_{oe,oo}^*} e^{-\frac{\alpha_{e,o}l}{2}} e^{j\beta_{e,o}l} \end{bmatrix} \begin{bmatrix} I_{1e,o}^+ \\ V_{1e,o}^- \end{bmatrix}$$

$$\therefore \begin{bmatrix} I_{1e,o}^+ \\ V_{1e,o}^- \end{bmatrix} = A_2^{-1} \begin{bmatrix} V_{2e,o} \\ I_{2e,o} \end{bmatrix} \quad (25)$$

Where

$$A_2^{-1} = \frac{1}{Z_{oe,oo} + Z_{oe,oo}^*} \begin{bmatrix} e^{-\frac{\alpha_{e,o}l}{2}} e^{j\beta_{e,o}l} & Z_{oe,oo}^* e^{\frac{\alpha_{e,o}l}{2}} e^{j\beta_{e,o}l} \\ Z_{oe,oo}^* e^{-\frac{\alpha_{e,o}l}{2}} e^{-j\beta_{e,o}l} & -Z_{oe,oo} e^{\frac{\alpha_{e,o}l}{2}} e^{-j\beta_{e,o}l} \end{bmatrix}$$

From matrix properties

$$\begin{bmatrix} V_{1e,o}^- \\ I_{1e,o}^- \end{bmatrix} = \frac{1}{Z_{oe,oo} + Z_{oe,oo}^*} \begin{bmatrix} Z_{oe,oo}^* e^{-\frac{\alpha_{e,o}l}{2}} e^{-j\beta_{e,o}l} & -e^{-\frac{\alpha_{e,o}l}{2}} e^{-j\beta_{e,o}l} \\ e^{-\frac{\alpha_{e,o}l}{2}} e^{j\beta_{e,o}l} & Z_{oe,oo}^* e^{\frac{\alpha_{e,o}l}{2}} e^{j\beta_{e,o}l} \end{bmatrix} \begin{bmatrix} V_{2e,o} \\ I_{2e,o} \end{bmatrix} \quad (26)$$

Where

$$V_{1e,o} = V_{1e,o}^+ + V_{1e,o}^- \text{ \& } I_{1e,o} = I_{1e,o}^+ + I_{1e,o}^-$$

$$\begin{bmatrix} V_{1e,o} \\ I_{1e,o} \end{bmatrix} = \begin{bmatrix} A_{e,o} & B_{e,o} \\ C_{e,o} & D_{e,o} \end{bmatrix}$$

Where

$$A_{e,o} = \frac{1}{Z_{oe,oo} + Z_{oe,oo}^*} (Z_{oe,oo} e^{j\beta_{e,o}l} + Z_{oe,oo}^* e^{-j\beta_{e,o}l}) e^{-\frac{\alpha_{e,o}l}{2}}$$

$$B_{e,o} = \frac{1}{Z_{oe,oo} + Z_{oe,oo}^*} (Z_{oe,oo} Z_{oe,oo}^* e^{\frac{\alpha_{e,o}l}{2}}) (e^{j\beta_{e,o}l} - e^{-j\beta_{e,o}l})$$

$$= \frac{1}{Z_{oe,oo} + Z_{oe,oo}^*} (Z_{oe,oo} Z_{oe,oo}^* e^{\frac{\alpha_{e,o}l}{2}}) (2j \sin \beta_{e,o} l)$$

$$C_{e,o} = \frac{1}{Z_{oe,oo} + Z_{oe,oo}^*} (Z_{oe,oo} Z_{oe,oo}^* e^{-\frac{\alpha_{e,o}l}{2}}) (e^{j\beta_{e,o}l} - e^{-j\beta_{e,o}l})$$

$$= \frac{1}{Z_{oe,oo} + Z_{oe,oo}^*} (Z_{oe,oo} Z_{oe,oo}^* e^{-\frac{\alpha_{e,o}l}{2}}) (2j \sin \beta_{e,o} l)$$

$$D_{e,o} = \frac{1}{Z_{oe,oo} + Z_{oe,oo}^*} (Z_{oe,oo} e^{-j\beta_{e,o}l} + Z_{oe,oo}^* e^{j\beta_{e,o}l}) e^{\frac{\alpha_{e,o}l}{2}}$$

4. The Scattering Matrix Parameters

First of all the even and odd mode $A_{e,o}, B_{e,o}, C_{e,o}, D_{e,o}$ matrices for the lossy non-uniform coupled lines must be derived. These are then used to calculate the reflection and transmission coefficients, in terms of which the scattering parameter matrix can then be written. The even and odd mode reflection and transmission coefficients for the non-uniform directional couplers are obtained as:-

$$\rho_{e,o} = \frac{Z_{L_{e,o}} A_{e,o} + B_{e,o} - Z_{L_{e,o}} Z_{S_{e,o}} C_{e,o} - Z_{S_{e,o}} D_{e,o}}{Z_{L_{e,o}} A_{e,o} + B_{e,o} + Z_{L_{e,o}} Z_{S_{e,o}} C_{e,o} + Z_{S_{e,o}} D_{e,o}} \quad (27)$$

$$\tau_{e,o} = \frac{2\sqrt{Z_{L_{e,o}} Z_{S_{e,o}}}}{Z_{L_{e,o}} A_{e,o} + B_{e,o} + Z_{L_{e,o}} Z_{S_{e,o}} C_{e,o} + Z_{S_{e,o}} D_{e,o}} \quad (28)$$

The scattering parameters for CBTL when the input signal either introduced at port (1) or port (2) (fig. 1) may be expressed as:

$$S_{22} = S_{11} = \frac{1}{2}\rho_e + \frac{1}{2}\rho_o \quad (29)$$

$$S_{12} = S_{21} = \frac{1}{2}\tau_e + \frac{1}{2}\tau_o \quad (30)$$

$$S_{42} = S_{31} = \frac{1}{2}\rho_e - \frac{1}{2}\rho_o \quad (31)$$

$$S_{32} = S_{41} = \frac{1}{2}\tau_e - \frac{1}{2}\tau_o \quad (32)$$

The same procedure can be applied in calculating the scattering parameters when the input signals are applied at either port (3) or (4).

5. Determination of Exponential Microstrip Coupled Line Parameters

Usually in designing procedure of the exponential microstrip coupled lines, the parameters, which are characterizing these structures, must be determined. These parameters include the even and odd mode capacitances, impedances, effective dielectric constants and phase velocities of propagation.

5-1 Calculation of the Even and Odd Mode Capacitances

Ramesh and Bahi derive expressions for the even and odd mode capacitances respectively as: [11]. see fig. 2.

$$C_e = C_p + C_f + C_f' \quad (33)$$

$$C_o = C_p + C_f + C_{ga} + C_{gd} \quad (34)$$

Where

$$C_p = \frac{\epsilon_o \epsilon_r W}{h} \quad (35)$$

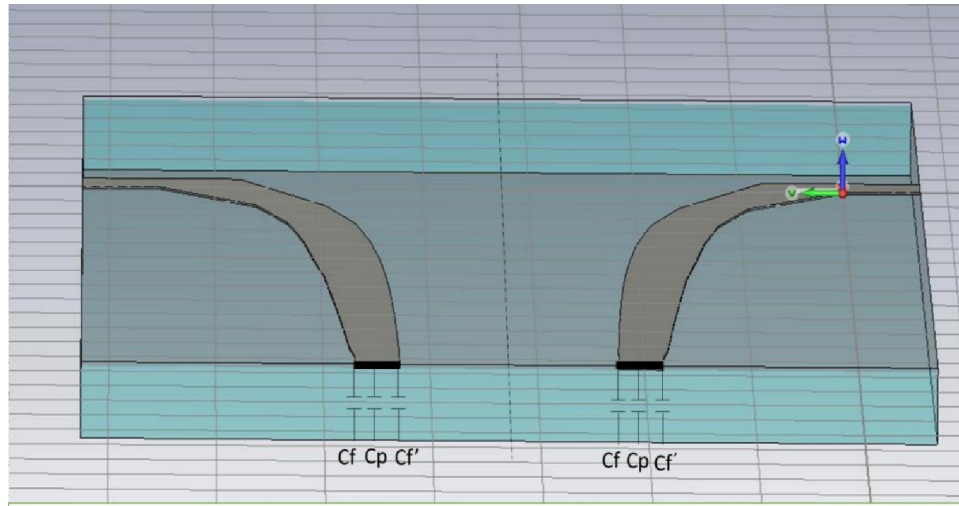


Fig.2a show the capacitances representation of the even mode field distribution for zero conductor thickness

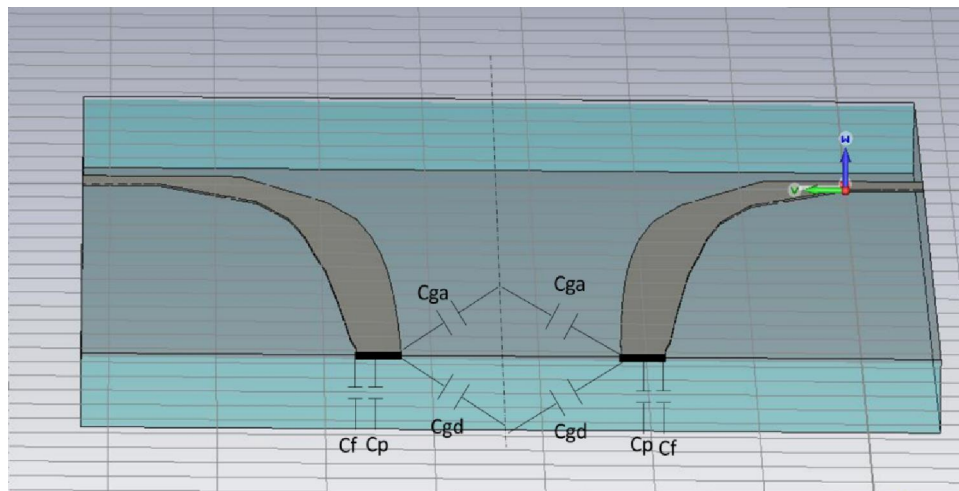


Fig.2b show the capacitances representation of the odd mode field distribution for zero conductor thickness

Where $\epsilon_o = 2.25 \times 10^{-4} \frac{pF}{cm} \epsilon_r$ = the dielectric constant of the material under investigations. While C_f, C_f', C_{ga} and C_{gd} were calculated and defined in reference [12].

Fig. 2 illustrates the capacitances representation of the even and odd mode electrical field distribution W and h are the width of the single conductor and the thickness of the substrate respectively. Saed Al-

Bodare improved equation (34) [2] by adding the fringing capacitance C_f' to the odd mode equation.

Fig. 3 show the capacitances representation of the improved odd mode electrical field distribution with C_f' is included.

$$C_o = C_p + C_f + C_f' + C_{ga} + C_{gd} \quad (36)$$

Where C_f' is the fringing capacitances, which was derived and defined in reference [13], [15].

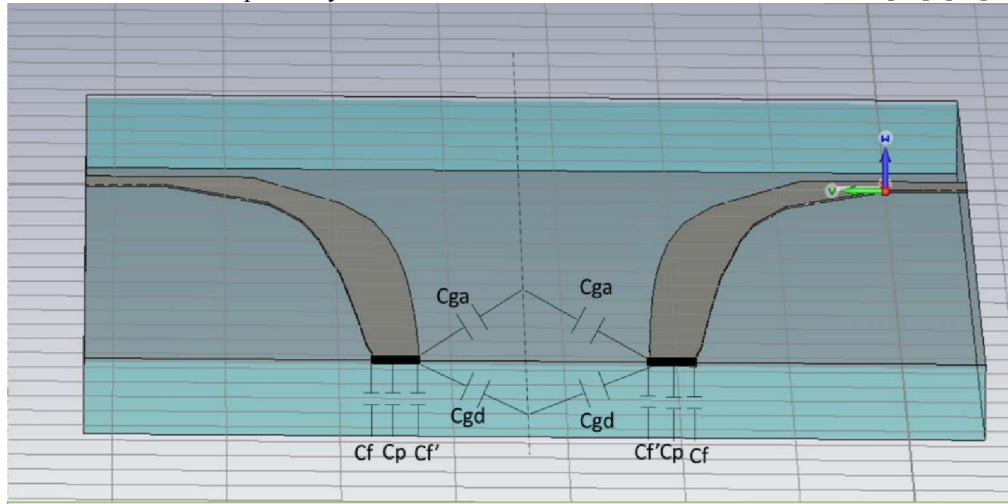


Fig. 3. The odd mode capacitance representation of the electric field distribution for zero conductor thickness.

Further improvement to equations (1) and (2) have been made by Dalby A.B. [14] by including the extra fringing capacitance which was caused by non-zero conductor thickness, See fig.4.

Therefore equations (33) and (36) can be written [16] as:

$$C_e = C_p + C_f + C_f' + C_f'' \quad (37)$$

$$C_o = C_p + C_f + C_f' + C_f'' + C_{ga} + C_{gd} \quad (38)$$

Where C_f'' was defined and derived in reference [17]. Also further improvement has been made to equation (32) by including the extra odd mode air capacitance, which was also attributed to the non-zero conductor thickness [6]. Therefore equation (32) becomes as:

$$C_o = C_p + C_f + C_f' + C_f'' + C_t + C_{ga} + C_{gd} \quad (39)$$

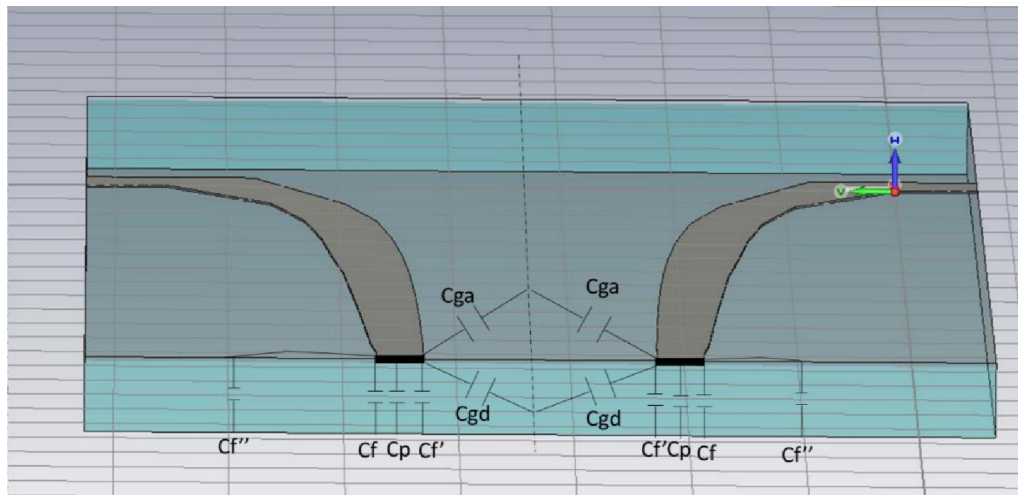


Fig. 4. Improved capacitor representation of the odd mode electric field distribution.

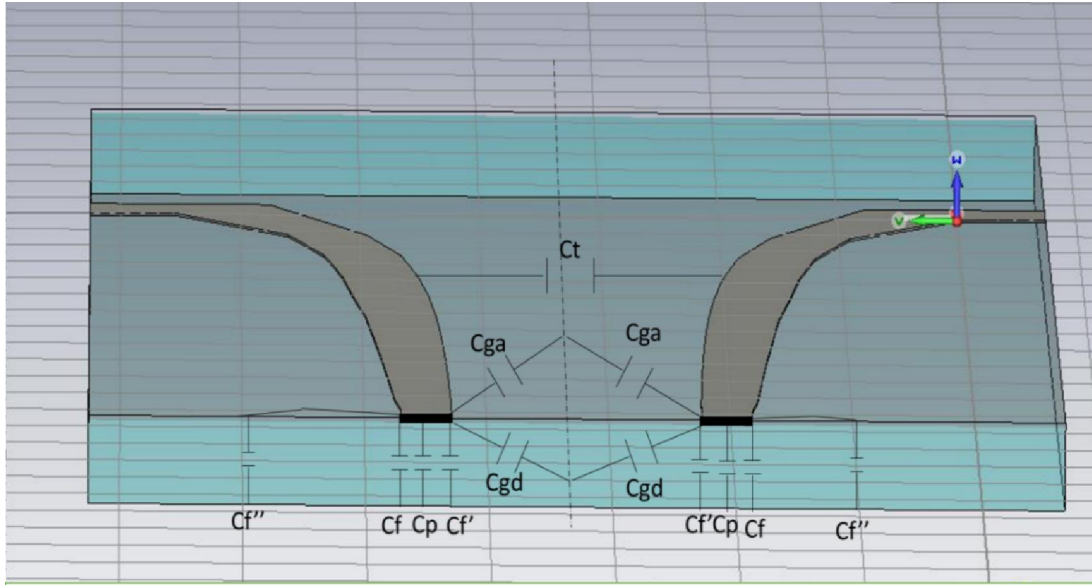


Fig.5. The extra improvement in the odd mode electric field distribution.

Fig. 4 shows the accurate decomposition of the odd mode capacitances. Where C_t is the increase in odd mode air capacitance, which can be written for the uniform, coupled line as:

$$C_t = \frac{\epsilon_o T L}{S} \quad (40)$$

Where T is the finite thickness of the conductor, L is the length of the conductor and S is the separation between the coupled lines. Equation (35) can be modified for non-uniform coupled lines as:

$$C_{t \text{ nonuniform}} = \frac{\epsilon_o T L}{\sum_{n=0}^{100} [S_o \pm n(2\Delta S_n)]} \quad (41)$$

Where the positive sign of $+2\Delta S_n$ indicates the incremental increase in the spacing between the coupled line obtained at the tight coupling end while the negative sign of $-2\Delta S_n$ indicates the incremental decrease in the spacing as one move from the loose coupling side to the tight coupling end.

Fig 5 shows how the computation of the spacing between the non-uniform coupled line has been done.

5.3 The Even and the Odd Mode Characteristic Impedances

The characteristic impedances for the two modes can be obtained from the capacitance value, using the following relations [14].

$$Z_{oe} = \frac{1}{V\sqrt{C_e C_e^a}} \quad (42)$$

$$Z_{oo} = \frac{1}{V\sqrt{C_o C_o^a}} \quad (42)$$

Where V is the velocity of the waves in air, while C_e^a and C_o^a denotes the even and odd capacitances with air as dielectric.

5.4 The Even and Odd Mode Effective Dielectric Constants

The effective dielectric constants of the even and odd mode can be expressed as: [18]

$$\epsilon^e r e = \frac{C_e}{C_e^a} \quad (43)$$

$$\epsilon^o r e = \frac{C_o}{C_o^a} \quad (44)$$

The hybrid effective dielectric constant may be written as: [19]

$$\epsilon e f f = \left(\frac{\sqrt{\epsilon^e r e} + \sqrt{\epsilon^o r e}}{2} \right)^2 + 0.082 \quad (45)$$

Once the material substrate is defined and the even and odd mode capacitances are computed, the cross sectional area dimension of the non-uniform couplers can be easily calculated at the central frequency as:

$$L = \frac{\lambda_o}{4\sqrt{\epsilon e f f}} \quad (46)$$

Where λ_o is the free space wave length.

6. General design procedure

In microstrip, the nonuniform coupled lines, are faced with the problem of different phase velocities or the even and odd modes of propagation. In microstrip coupled lines, uniform or nonuniform, the inequality in the phase velocities of the even and odd mode usually raised several problems i.e. low directivity and return loss. Therefore a perfect coupler with perfect matching and infinite directivity is not achievable in practice. Thus the amount of parameter tolerance need to be specified in the initial stage of directional coupler design.

The initial specifications for the required directional coupler are:

- 1) Coupling factor, say, $C = -10 \pm 0.45$ dB
- 2) Single microstrip feedline characteristic impedances $Z_o = 50 \Omega$
- 3) Substrate permittivity ϵ_r , and thickness of the substrate h
- 4) $\frac{T}{h}$ Ratio of the conductor thickness to substrate thickness.
- 5) Dielectric constant Teflon: $\epsilon_r = 2.3$ or Alumina: $\epsilon_r = 9.7$
- 6) The operating frequency $f_o = 12$ GHz
- 7) Lowest acceptable isolation $I = -30$ dB
- 8) Mismatch acceptable = -30 dB
- 9) Transmission $\tau = 0$ dB

The approximate condition for minimum input mismatch and maximum isolation is as follows [18]:

$$Z_o^2 = Z_{oe}(x) * Z_{oo}(x) \tag{47}$$

7. Design procedure for Exponential taper directional coupler

In the design of an exponential directional coupler one can assume that the equation (42) is satisfied, if the even and odd modes rate of taper are chosen to be

$$\delta_e = -\delta_o \tag{48}$$

or vice-versa.

Therefore the condition for best performance of the proposed coupler becomes

$$Z_o^2 = Z_{oe} e^{\delta_e x} * Z_{oo} e^{\delta_o x} \tag{49}$$

8. The Performance of The Coupled Exponential Directional Couplers

The CETL directional couplers were designed on three identical substrates of dielectric constant $\epsilon_r = 10$ and thickness $h = 0.635$ mm with coupling specification of 10.25 ± 0.45 dB. These couplers were designed to operate at 3.5 GHz with acceptable bandwidth of 10%. The typical frequency responses of the computed and measured scattering matrix-parameters of $S_{11}, S_{21}, S_{31}, S_{41}$ and $S_{14}, S_{24}, S_{34}, S_{44}$, when the input signals were introduced at ports (1) and (4) respectively. Because of the symmetry, the remaining scattering matrix parameters of $S_{12},$

S_{22}, S_{32}, S_{42} and $S_{13}, S_{23}, S_{33}, S_{34}$ where the input signal were applied at ports (2) and (3) respectively are not required. Fig. 5 show very good agreement of the optimized values were obtained. The optimized theoretical frequency responses of the scattering matrix parameters $S_{11}, S_{21}, S_{31}, S_{41}$ and S_{14}, S_{24}, S_{34} and S_{44} of the exponential directional coupler were compared with the published work in reference [1] and they were found to be in good agreement only with the scattering matrix parameters resulted from excitation of the CETL coupler at either ports (1) or (2), while the scattering matrix parameters resulted from the excitation signal at either port (3) or

(4) were found to be different from that of reference [2] and this was due to the incorrect substitution of the values of the even and odd mode characteristic impedance CETL parameters in[2]. At high frequencies, the isolations of the proposed non-uniformed directional couplers deteriorate due to the difference in the even and odd mode velocities.

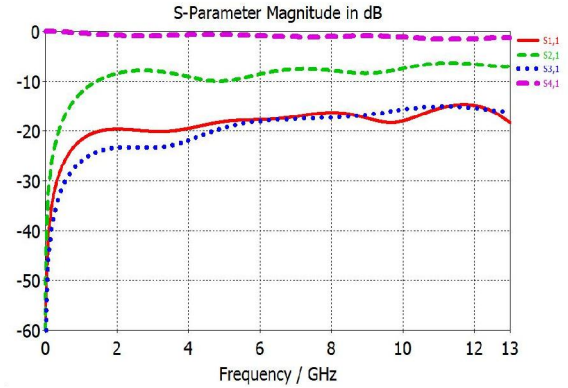


Fig. 6. The scattering parameters $S_{11}, S_{21}, S_{31}, S_{41}$ of a CETL directional coupler in an inhomogeneous medium.

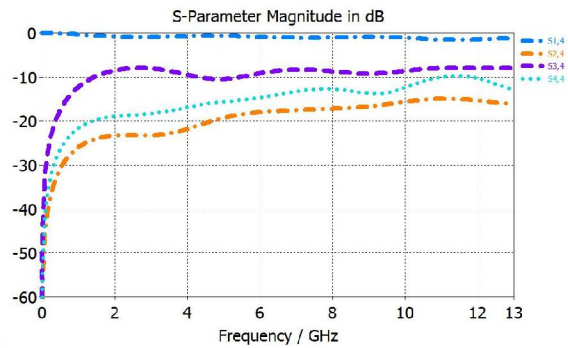


Fig. 7. The scattering parameters $S_{14}, S_{24}, S_{34}, S_{44}$ of a CETL directional coupler in an inhomogeneous medium.

9. Development of Neural Network

Neural network as the name sounds is interconnection of nerve cells. The artificial neural network technology is built up with an inspiration of functioning of human nervous system. Many of human intelligent behavior which is the direct functioning of human nervous system are implemented artificially in artificial neural network. It is inspired by the way biological nervous systems works. It is composed of a large number of highly interconnected processing elements called neurons working in union to solve specific problems. Like human, artificial neural network also learn by example. It is configured for specific application, such as pattern recognition or data classification through learning process. Learning involves adjustments to the synaptic connection known as weights that exist

between the neuron. In artificial neural network, the information processing elements are known as nodes. The first layer of nodes is known as input layer. Whereas the last layer is known as output layer. The layers in between which may or may not exist is known as hidden layer(s). The information is transmitted by means of connecting links. The links possess an associated weight, which is multiplied with the incoming signal for any typical neural network. The output is obtained by applying activations to the net. Artificial neural network is used to train computers to do various operations which need human intelligence. There are various categories of artificial neural networks used for training computers for specific category of work. Among the single layered networks there are Perceptron Model, Associative Network, Adaline Network, Madaline Network, Hofffield Network whereas in multilayered network we have Back Propagation model, radial basis network, self organizing map, learning vector quantization etc[20].

9.1 Estimation of Exponential Directional Coupler TL

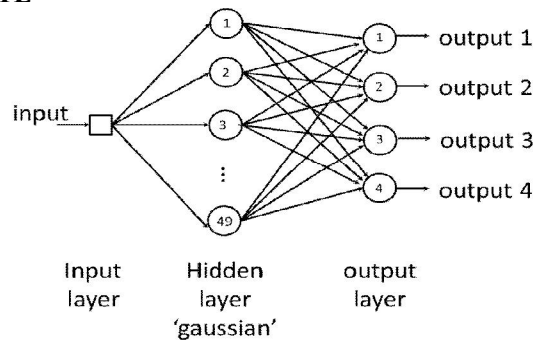


Fig. 8. RBFNN algorithm (2) recursive

Radial Basis Function Neural Networks (RBFNN) algorithm (2) recursive is used to estimate exponential directional coupler transmission line. The construction of RBF network, in its most basic form, involves three layers with entirely different roles. The input layer is made up of source nodes (sensory units) that connect the network to its environment. The second layer, the only hidden layer in the network applies a nonlinear transformation from the input space to the hidden space. In most applications the hidden space is of high dimensionality. The output layer is linear, supplying the response of the network to the activation pattern applied to the input layer. A RBF net architecture is given in figure 8. Radial Basis function networks are substantially faster than the methods used to train multi-layer perceptron networks. This follows from the interpretations which can be given to the internal representation formed by the hidden units, and leads to a two stage training

procedure. In the first stage, the parameters governing the basis functions (corresponding to hidden units) are determined using relatively fast, unsupervised methods, in which it uses only input data and not the target data. The second stage of training then involves the determination of the final-layer weights, which requires the solution of a linear problem, and which is therefore also fast. The trained neural network provides a special approximation where the exact results of the numerical analysis, which are hidden in the training patterns, are used for neural computation and give us directly all the required designing parameter of an antenna for a desired frequency. That way, a computationally modest neural network model can replace a numerical analysis for parameters differing from training patterns.

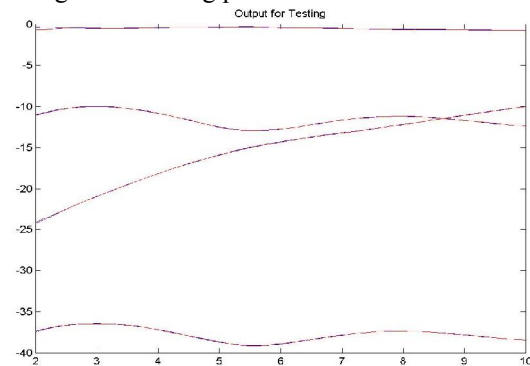


Fig. 9. The scattering parameters of [1] and Estimation.

9.2 RBFNN algorithm (2) recursive Architecture

In fig 8 first layer is called as input layer where external information is received and is consisted of 1 input frequency f in GHz. The middle layer consist of 49 neurals with Gaussian activation function. The last layer is called as output layer where the network produces the model estimation and is consisted of 4 outputs and S_{11} , S_{21} , S_{31} and S_{41} . Fig. 8 shows the result of estimation graph. The accuracy of the RBFNN technique was evaluated by comparing the predicted solutions from our neural network to those from a published paper [1]. Fig. 8 show an excellent agreement between the results provided by Koboyashi K., Nemoto Y [1] and the RBFNN.

9.3 Finding physical dimensions using Optimization and Neural Network

In this paper, two types of neural network have been used to find the physical dimensions of the exponential directional coupler (w/h and s/h). First type is Radial.

Basis Function Neural Networks (RBFNN) algorithm (3). Architecture structure is shown in fig, 12. Second type is Back Propagation neural network (BPNN). For designing this type of neural network we use nntool in matlab software. Architecture structure

is shown in fig, 13. RBFNN algorithm (3) in fig. 10 consists of 3 layers. First layer is called as input layer where Z_{eo} and Z_{oo} are received. The middle layer consist of 101 neurals with Gaussian activation function. The output layer is consisted of 2 neurals w/h and s/h . BPNN in fig. 13 is consist of 3 layers. The input layer has 2 neurals Z_{eo} and Z_{oo} . The middle layer is made of three hidden layers and 10 neurals in each hidden layer with tensing activation function. The output layer is consisted of 2 neurals w/h and s/h .

The both neural networks are trained with data set of various values of Z_{eo} , Z_{oo} , w/h and s/h including in table 1. Once you have trained the network, choose Z_{eo} , Z_{oo} to simulate, for which design parameters are to find, It can calculatr the design constraints close to optimum value of w/h and s/h . Simulated results are shown below(see fig.14).

The dimensions of EDCTL calculated by RBFNN and BPNN are very close to each other.

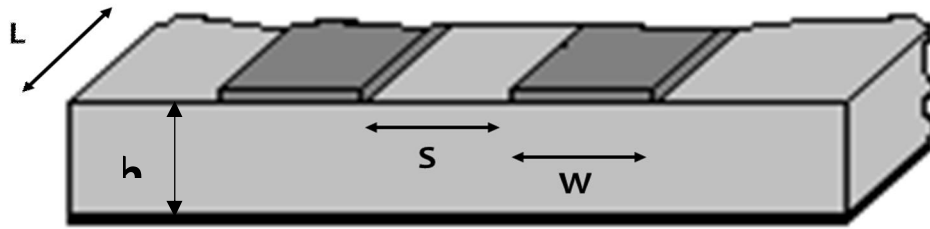


Fig. 10.physical dimensions of EDCTL

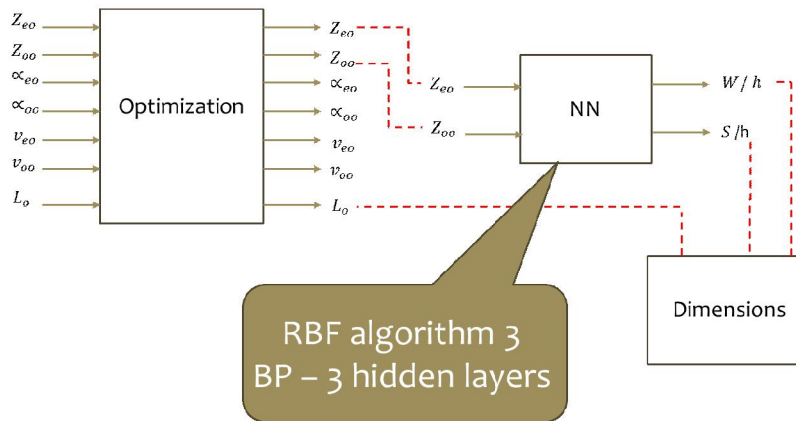


Fig. 11. Finding physical dimension using Optimization and Neural Network

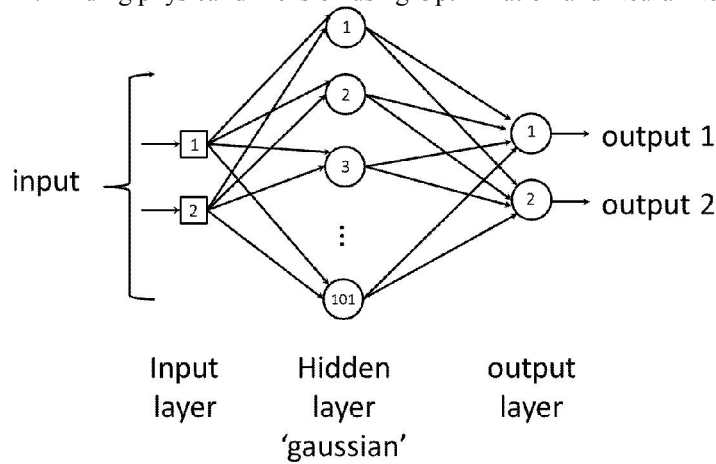


Fig. 12. RBFNN algorithm (3)

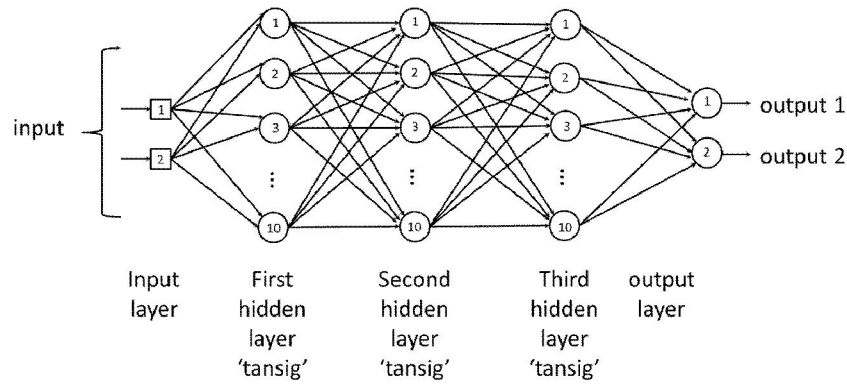
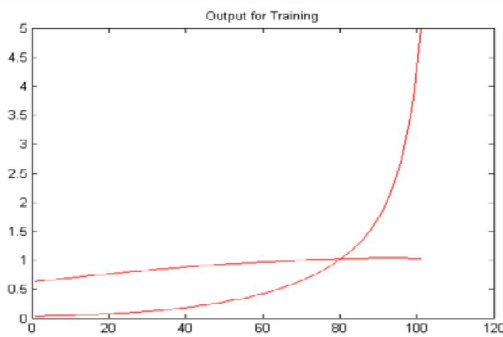
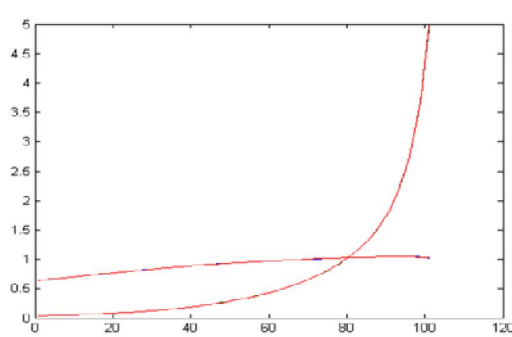


Fig. 13. BPNN



RBF

w/h = 1.5965 s/h = 0.1031 L = 2.5 mm For BPNN



BP

w/h = 1.5919 s/h = 0.1023 L = 2.5 mm

Fig. 14 The output of training of RBFNN and BPNN for RBFNN

Conclusion

The solution derived for the characterization of CETL in inhomogeneous media gives good design parameters for microwave couplers. Microstrip couplers using EDCTL have a much flatter frequency response than those using uniform lines. The use of neural network for transmission line analysis opens the way to a significant improvement in design efficiency. Moreover, nothing prevents this technique to be applied to more complex structures, like non-symmetric transmission line or even multi-mode waveguides. The analysis of nonuniform waveguides is a problem for which there are currently no simple and efficient solutions. The proposed technique has great potential to provide answers in this area. we have presented a technique to compute the scattering parameters of a nonuniform symmetrical transmission line by using an artificial neural network. Also in this work, the neural network is employed as a tool in design of the EDCTL. In this design procedure, synthesis is defined as the forward side. Therefore, one can obtain the geometric dimensions with high accuracy, i.e. w/h and s/h in our geometry, at the

output of the synthesis network by inputting Z_{eo} and Z_{oo} .

References

1. Koboyashi K., Nemoto Y., and Sato R." Equivalent circuits of binomial form non uniform transmission lines and their application," Trans. IECE, Japan, volume. 63-a, number (11);, pages. 807- 814, November 1980.
2. Sobhy M. I. and Hosny E. A."The design of directional couplers using exponential lines in homogeneous media "IEEE Trans. Microwave Theory Tech., volume. MTT-30, pages.:71-76, January. 1982.
3. Affandi A. M., Mahdi S., Almoabadi M.,"Analysis of some non-uniform transmission lines with selected applications" ICECS'94, pages. 153-162, December 19-22, 1994, Cairo, EGYPT.
4. Oiiita I., Kawai T., Shimahasih S., Ho K., " A Transmission line type eight port hybrid " IEEE. Trans. Microwave Theory Tech., volume. MTT- S Digest pages. 119 - 122, 1992.

5. Steven. L. March "Analyzing Lossy Radial - Line Stubs ", Microwave Theory Tech., volume. MTT-33, Number. 2, pages 269-271, March 1985. IEEE Transmission Line Theory, Waves, volume.128, Pt. H, Number.(2).; APRIL,1981.
6. Lacombe D. and Cohen J., "Octave - Band DC Blocks", IEEE Trans. Microwave Theory Teach. Volume MTT, pages. 55 - 56, August 1972.
7. Takada F. and Matsunaga M. "Small - Sized Diode Phase Shifter ", 11th EUMC, pages. 833 - 838, Amsterdam 1981.
8. Kumar S., Danshin T., "A Multisection Broadband Impedance Transforming Branch line Quad Hybrid Suitable for MMIC Realization" The international conference and exhibition designed for the microwave community proc., volume 2, pages: 1301- 1306, August 1992.
9. Meaney P., "A Novel Branch - Line Coupler Design For Millimeter - Wave Applications " IEEE MTT - S Digest, Number 0 - 4 pages 585 - 588, 1990.
10. Reed J. and Wheeler G. J., "A method of Analysis of symmetrical four port networks", RE. Trans. Microwave Theory Tech., volume. MTT-4, pages. 246-252, October. 1956.
11. Goerg R. and Bahi I. J., "Characteristics of Coupled microstriplines," IEEE Trans. Microwave Theory Theory Tech., volume. MTT-27, pages.700 - 704, 1979.
12. Jacobs I., "The non-uniform transmission line as a broadband termination " Bell ayst. Tech. J., pages. 913-924, July 1958.
13. Bedair S. S., "On The Odd Mode Capacitance Of The Coupled Microstrip Lines", IEEE Trans, Microwave Theory Tech., volume. MTT-28, pages. 1225 - 1227, 1980.
14. Walker L. R. and Wax N., " Non-Uniform Transmission Lines and Reflection Coefficients", Journal Of Applied Physics, volume 17, pages 1043-1045, December, 1946.
15. Alley G., "Interdigital capacitors for use in lumped element microwave integrated circuits" In Proc. IEEE. MTT Int Microwave Symp. pages 7 - 13 1970.
16. De Brecht R. and Caulton M., "Lumped Elements In Microwave Integrated Circuit 1 - 12 GHz range" In Proc, IEEE. G. MTT Int Microwave Symp., pages. 14 - 18 1970.
17. Harry A. A. " Microstrip Reavtive Circuit Elements ", IEEE Trans. Microwave Theory Theory Tech., volume. MTT-31, pages. 488 - 491, 1983.
18. Yamamoto S., Azakami T. and Itakura, K. "Coupled non-uniform transmission line and its applications, " IEEE Trans. Microwave Theory Tech., volume. MTT-15, Number. 4, pages. 220-231, April 1967.
19. Ho C. Y., " Analysis Of DC Blocks Using Coupled Lines ", IEEE. Trans. Microwave. Theory Tech., volume. - MTT, pages. 773 - 774 September. 1975.
20. Pandit M., T. Bose " Application of Neural Network Model for designing Circular Monopole Antenna " International Symposium on Devices MEMS, Intelligent Systems & Communication (ISDMISC) 2011. Proceedings published by International Journal of Computer Applications® (IJCA) pages. 18 – 21.

4/7/2015